Fabrication and Study on Red Light Micro-LED Displays

RAY-HUA HORNG [1,2] (Fellow, IEEE), **HUAN-YU CHIEN**[3], **FU-GOW TARNTAIR**[1],
AND DONG-SING WUU [4,5] (Senior Member, IEEE)

1 Institutes of Electronics, National Chiao Tung University, Hsinchu 300, Taiwan
2 Center for Emergent Functional Matter Science, National Chiao Tung University, Hsinchu 300, Taiwan
3 Graduate Institute of Precision Engineering, National Chung Hsing University, Taichung 402, Taiwan
4 Department of Materials Science and Engineering, National Chung Hsing University, Taichung 402, Taiwan
5 Innovation and Development Center of Sustainable Agriculture, National Chung Hsing University, Taichung 402, Taiwan

CORRESPONDING AUTHOR: R.-H. HORNG (e-mail: rhh@nctu.edu.tw)

ABSTRACT A red-light micro LED display made of an AlGaInP epilayer with a resolution of 64×32 pixels, a pitch of 175 μm and a luminous area of 1 cm $\times$ 0.5 cm was fabricated and characterized in this study. The AlGaInP epilayer was bonded to double polished sapphire substrate by wafer-bonding technique and then removing the absorbing GaAs substrate. In this design, the ITO was applied as one of the conducting electrodes of the emitting surface, which can be beneficial since the emitting light is not shielded by metal electrodes. The other key process for LED panel fabrication is planarization. Polymer material was used to fill the gap between each pixel, which was used to prevent a short or open circuit using the planarization process. The driving mode of this display is passive multi-electrode addressable controlling. The luminance of this micro-LED panel is more than 450 nits with an operating voltage of 3 V which is three times higher than that of the OLED operating in the same driving mode.

INDEX TERMS Micro-LED display, ITO electrode, passive mode panel.

I. INTRODUCTION

Compared with liquid crystal displays or organic LED displays (OLEDs), which are conventionally used as light sources for displays, displays made of inorganic LEDs have many merits such as high brightness, low power consumption, a short response time, high stability and long life [1]–[4]. In fact, using LEDs to play display applications is not new [5], [6]. LED TV walls for advertisements have been used for a long time. However, the resolution for this kind of application is always low. Recently, the efficiency of LEDs has become high and semiconductor fabrication is more mature. Thus, high resolution displays made of LEDs is the most advanced, low-power optoelectronics capability currently on market and can dynamically change any text or icon. [7], [8]. Micro-displays (μD) made of LED arrays are a type of LED device that shows promising technology for many applications, like self-emissive displays, automotive, wearable devices, military applications, biologic transducers,

optical biological chips, medical treatment, etc. Different results have been successively reported using GaN/InGaN LED material with promising electro-optical properties of μLED matrices, which suggests that there is a high potential for μD applications [2], [9], [10]. Although the use of an active matrix to individually control each μLED pixel has been demonstrated on a large scale 640×480 pixel matrix with a 15 μm pitch, it paves the way towards high resolution and efficient μLED μDs [2]. Today, active-matrix displays are fabricated using thin-film transistor (TFT) technology. However, TFT technology encounters the challenge about the requirements in true emissive displays where the pixel circuit must supply an accurate and uniform electrical drive current to each emissive element in the display instead of just driving a voltage-controlled switch. Moreover, the precision alignment of the μLED and TFT should be required and increase the fabrication cost. However, there is another choice, i.e., combined with a passive matrix driver, μDs are

attracting more attention with interconnect processing which has many advantages, such as easy fabrication and low cost. Nevertheless, most µDs are focused on the blue and green lights made by GaN-based LEDs due to the transparent epitaxial substrate and insulating sapphire substrate [11]. Red light µD has seldom been reported because the material of the red-light LED is AlGaInP grown on opaque and conductive GaAs substrate. Because there are many important applications for the red-light µD, e.g., red-light µD can project important information in the helmet, ensuring that pilots can receive it under the sunny day. They can also be applied to other security display like the automobile, smart watch, smart keyboard and smart home appliances. In this study, we developed a passive matrix µD (the size of each red LED pixel: 100 µm×100 µm), with a resolution of 64 × 32 pixels, a pitch of 175 µm, as well as a 1 cm × 0.5 cm luminous area. The passive matrix driver offers 3V (2.8-3.3 V) and 1/32 duty cycle. The LEDs which were applied in this panel were red AlGaInP-based LEDs. In our previous study [12], the light cross talk can be suppression about 80 µm. So the cross talk is not so serious in this display.

Moreover, the AlGaInP epilayer with an ITO transparent contact layer was bonded to the double polished sapphire substrate by wafer-bonding technique [13], [14] and then removing the absorb GaAs substrate. In this design, the ITO was applied as one of the conducting electrodes of the emitting surface, which can be beneficial since the emitting light is not shielded by metal electrodes. Compared to a traditional metal electrode, there is no emitting light shielding issue in this design, and this reveals that the resolution of the display was enhanced and the current distribution was more uniform using this kind of structure. Another key process for LED panel fabrication is planarization. A polymer was used to fill the gap between each pixel allowing the short or open circuit to be eliminated by the planarization process. It should be pointed out that the performance of an LED panel is influenced by the uniformity and height of planarization. Processing and the performance of µDs will be discussed in detail in the following.

II. EXPERIMENTAL SECTION

AlGaInP LED epilayers were grown on n-type lattice-matched GaAs substrates by metalorganic chemical vapor deposition [14]. Then, an ITO layer was deposited on the epilayers of an AlGaInP LED using an E-Gun evaporator for Ohmic contact and current spreading, as shown in Fig. 1(a). Thermal anneal treatment was processed for Ohmic contact between the ITO and 1.0 µm thick p-GaP. Second, glue was used to bond the epilayers depositing ITO on double sides of the polished sapphire substrate, as shown Fig. 1(b). Next, the GaAs substrate was removed to expose the n-type AlInP layer by wet chemical etching, as shown in Fig. 1(c).

Following, the n-metal electrodes were defined by photolithography; the 64(Column with the same ITO line)×32(Row with the n-metal connetion) pixel array was
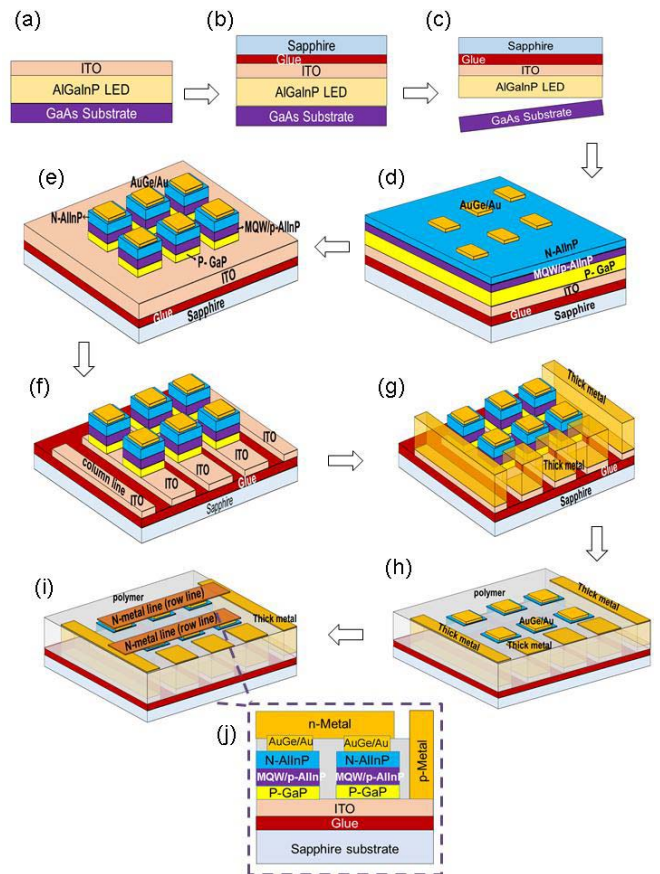

FIGURE 1. Process flow of 32 × 64 pixels micro LED display panel: (a) ITO Deposited by E-Gun evaporator, (b) Sapphire bonded by wafer bonding, (c) GaAs substrate removed by etching, (d) AuGe/Au deposited by thermal deposition system, (e) Epilayer etching to ITO, (f) ITO isolated by etching, (g) Metal deposited by E-Gun evaporator, (h) Fill and level up to groove by polymer, (i) Column metal line deposited by E-Gun evaporator, and (j) a side view diagram of the layer structure of the final display.

defined in this step. After this, n-metal AuGe/Au was deposited on the surface of the exposed n-type AlInP and photoresist. The N-metal region was formed after the lift-off steps, depicted in Fig. 1(d). The thermal anneal was treated for Ohmic contact between the AuGe/Au metal and n-type AlInP. Following this, the mesa isolation area with a 64×32 array was defined, and the mesa region was formed and stopped at the ITO layer by dry etching, as shown in Fig. 1(e).

After the LED mesa was formed, the address electrodes and panel circuits were defined in the following steps. The ITO was used as one of the electrodes to interconnect the LEDs in 32 rows of the 64 × 32 array for the addressing control in the panel. The etching depth of the ITO was about 200 nm, and the etching was stopped at the adhesive layer, as shown in Fig. 1 (f).

Before the column circuits were fabricated, there existed very high gaps between the LED chips and ITO electrode. These open regions would result in the line being broken for the metal line deposition to define the column address

interconnections. Thus, the metal plateau must be fabricated to prevent the open circuit issue and to form the metal contact for the next column electrode fabrication. The height of the metal plateaus should be the same as that of LED chips. These metal plateaus, defined by photolithography and multi-layers with Ti/Al/Ti/Au (50 nm/2.6 μm/50 nm/60 nm), were deposited by an E-Gun evaporator. The metal plateaus were formed by a lift-off process, as shown in Fig. 1(g).

The row address metal electrodes and circuits are fabricated in the next procedures. However, there existed very high gaps between the LEDs and substrates. The same issue of open circuits will easily happen due to the gap. To prevent this issue, the planarization process was considered. Polymer material was used to flatten the surface for the overall panel, as shown in Fig. 1(h). The ITO was used as one of the electrodes for the LED row address control described in the previous procedures. As the planarization process was completed in Fig. 1(h), the metal electrodes for the row address controlling of the LED array was achieved by photolithography definition first. Then, the metal layers of Ti/Al/Ti/Au (50 nm/2.3 μm/50 nm/60 nm) were deposited by tan E-Gun evaporator. Finally, the address metal electrodes for the 32 controlled rows were obtained after PR lift-off, shown in Fig. 1 (i). Fig. 1(j) shows a side view diagram of the layer structure of the final display. The final process is to connect the ITO circuit to the peripheral control circuit. Here, the bonding metal was used to combine the ITO electrode and peripheral circuit. Besides, this bonding metal can reduce the series resistance of the ITO. The bonding metal was also defined by photolithography. Then, the Cr/Au metal layer was deposited by a thermal evaporator. Fig. 2 shows the picture of the micro display after processing.
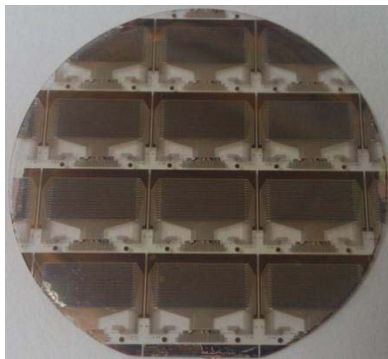

FIGURE 2. Picture of micro display fabricated by 2″ epiwafer after processing.

III. RESULTS AND DISCUSSION

In this study, we developed a multi-line addressable passive micro-LED display with the 64 column and 32 row control lines fabricated by ITO and metal lines, respectively. For a passive driven mode panel, it is necessary to evaluate whether the optoelectronic performance of each pixel is affected by the series resistance of the address lines.

Based on Equation (1), the series resistance was higher if the conducted path length was longer. The luminance of the LED was dependent on the driving current. The farther the distance from the p-contact metal, the higher the series resistance. This would result in a lower luminance of the μDs. The schematic diagram of the current path through the row line is shown in Fig. 3(a), and the equivalent circuit diagram is shown in Fig. 3 (b).
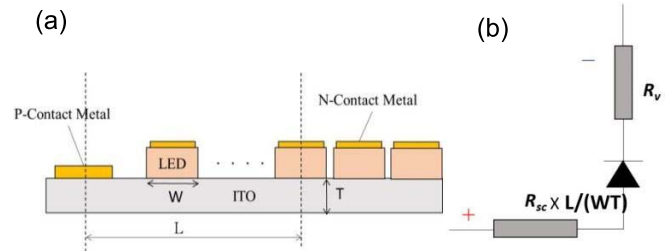
$$Rs = Rv + Rsc \times L/(WT) \tag{1}$$

FIGURE 3. (a) Schematic diagrams of current path through the column line, and (b) the equivalent circuit diagram.

Here, Rs is the series resistance, Rv is the resistance of the pixel and Rsc is the sheet resistance of the ITO and the metal stack. L is the distance between the pixel and the p-contact metal pads. W and T are the width and thickness of the ITO or metal, respectively.

The luminance uniformity of each LED is important for display application. The electrical properties of 64×32 micro-LEDs were analyzed. We measured the I-V characteristics of the LEDs for each pixel on a single column line, as shown in Fig. 4 (a). It was found that the series resistance values of pixels were increased from 0.089 Ω to 0.5 Ω for pixels located in row 1 to row 32. The serious increase in the Rs resulted from the current flowing through the thin ITO column. Here, the thickness of the ITO was only 200 nm. This problem can be overcome by increasing the thickness of ITO, GaP remaining on ITO or deposited metal on ITO. They are important and under study. On the other hand, the I-V characteristics of the LED for each pixel on a single row line was measured and is shown in Fig. 4 (b). It was found that the Rs variation is less dependent of the column position. This could be due to the fact that the current flows from the ITO/LED pixel and n-metal electrodes. Since the metal resistance is very low, it would not change the Rs very much for the I-V characteristic of the pixel located in the same row. The Rs variation could be attributed to the quality variation of the Ohmic contact between the metal and the n-AlGaInP epilayer.

Furthermore, we selected 3 columns and 3 rows to measure the I-V characteristics to realize the electrical performance of the whole display panel. The three columns were columns 3, 33 and 61. The forward voltage (V_f) variation from p-contact electrode ITO to each row pixel (1 to 32) was measured under injection current 1 mA. The schematic diagram of the three columns for measurement is shown in the inset in
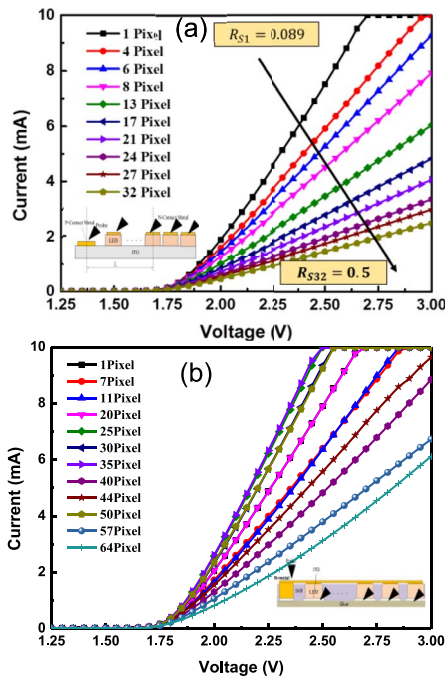
FIGURE 4. (a) I-V curves of pixels in a single column, (b) I-V curves of pixels in a single row.

Fig. 5 (a). It can be clearly observed that the V_f becomes a little higher as the row pixel position is located farther away from the ITO p-contact electrode. The V_f varied for these three columns from 1.9 to 2.2 V for the LED pixel located in rows 1 to 32, respectively. It was also found that the variety tendency was the same as those for the same row pixels located in different column lines. The increase in V_f is caused by the ITO series resistance. Furthermore, it was found that some pixels located in rows (12, 15 and 25) showed a higher V_f than the others. This could be due to the Ohmic contact properties not being as good as those of other pixels.

On the other hand, we investigated the electrical behavior of pixels for a row line with different columns. Rows 3, 15 and 31 were selected to check the V_f variation from metal contact with each column pixel under the same injection current 1 mA, as shown in Fig. 5 (b). The schematic diagram of these rows with different columns for electrical measurement was shown in the inset of Fig. 5(b). It was found that for the pixels located in higher columns, the current will flow into longer metal. Nevertheless, the V_f did not change significantly due to the row's low series resistance. This result coincided with that shown in Fig. 3(b). Furthermore, the voltages of pixels located in Row 31 presented as higher than those of pixels located in Row 15. The lowest pixel voltages were located in Row 3. The results agreed well with those of Fig. 4.

As mentioned, the display in this study was a passive driving mode panel. The optoelectronic performances of LED pixels would be affected by the series resistance. Here, it
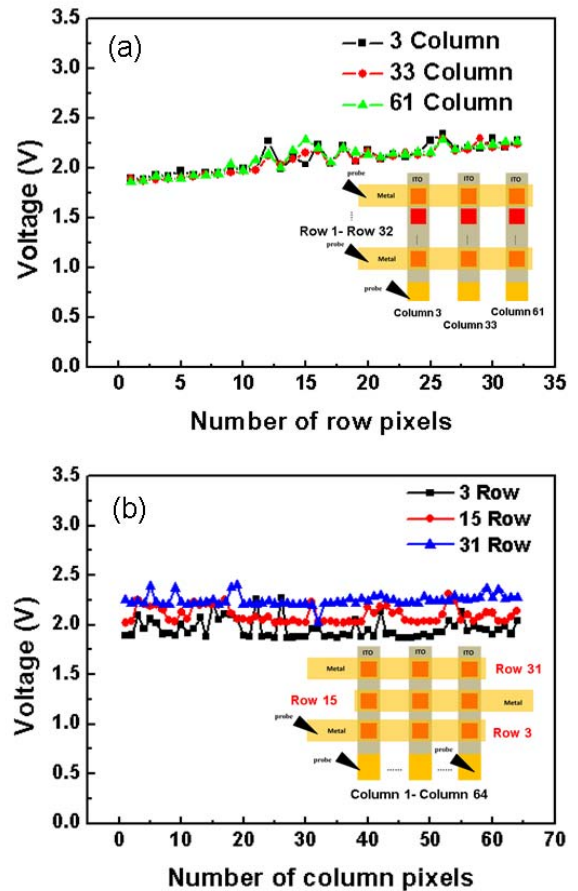

FIGURE 5. (a) V_f variations in the row pixels in three individual columns. Inset is the schematic diagram of measurement for the three columns, (b) V_f variations in the columns pixels in three individual rows. Inset is the schematic diagram of measurement for the three individual rows.
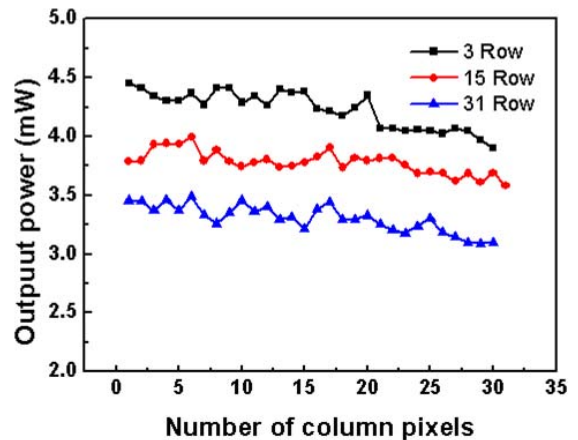

FIGURE 6. Light output power of LEDs located in the row pixels in three individual columns.

is important to measure the emission light of LEDs with the 3 columns and 3 rows under a driving current of 1 mA. Fig. 6 shows the output power of each row pixel for columns 3, 33 and 61. The output power decayed with the increase in the distance of pixel to p-contact, which was
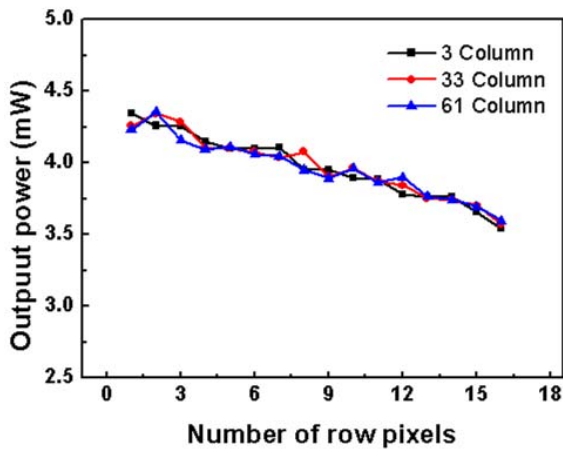
FIGURE 7. Light output power of LEDs located in the column pixels in three individual rows.

FIGURE 9. Photos showing the micro-LED display in this study.

current increased. The 464 nits maximum brightness could be obtained when the driving current was at 48 mA. The performance was better than that of a commercially available OLED display of the same size. The photo of this panel is shown in the inset of Fig. 8 where all of the LEDs were turned on. Fig. 9 also demonstrates some photos of the information shown by this micro LED display.

IV. CONCLUSION

In this study, we have demonstrated a red-light micro-LED display with a resolution of 64×32 pixels with a pitch of 175 μm and a panel size of 1 cm $\times$0.5 cm. In this design, the epilayer of LEDs was transferred to a transparent sapphire substrate using a wafer bonding technique. The ITO was applied as one of the conducting electrodes of the illumination surface, creating the benefit that the emitting light is not shielded by metal electrodes compared to a traditional LED. To analyze the I-V characteristics, the V_f of the LEDs in a column line were increased as the distance of the pixel to p-contact metal was increased, and there was a 28.7% forward voltage variation in the 5.6 mm display panel. However, this same phenomenon was not observed in the rows. The major reason was that the series of ITO column lines were higher than the metal row lines. The output power of LEDs also showed the same effect in the column pixels, but no issues were observed. It also should be pointed out that the planarization process was a key parameter to the uniformity of LED output power in this display. The overall output of the display panel was also measured, and the maximum, minimum and average values were 4.45 mW, 3.09 mW and 3.84 mW. There was a 44% output variation in the 1 cm $\times$0.5 cm display panel. The brightness of the micro LED display went up to 464 nits as the driving current increased to 48 mA which meant that the performance can be competed with a commercially available OLED display of the same size.
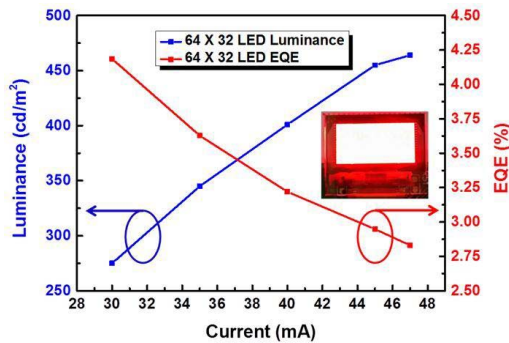

FIGURE 8. Luminance and EQE of micro LED panel as a function of the driving current, all LEDs in the panel were turned on, as shown in the photo of the insert.

obviously caused by the series resistance increase as the distance of the row pixel to p-contact increased. It is worthy to mention that the output powers of pixels located in different columns but in the same row appear almost the same. On the other hand, the output powers of pixels located in rows 3, 15 and 31 were also measured under the same driving current and are shown in Fig. 7. The output power of the three rows also decayed with the increase in the distance of the pixel to the metal contact, but it was not as serious as the output power behavior of the column pixels. This could be attributed to the series resistance of the metal line being low and not changing as much as the increase in the distance of the pixel to the metal contact. The overall output of the display panel was also measured; the maximum, minimum and average value were 4.45 mW, 3.09 mW and 3.84 mW. There was a 44% output variation in the 1 cm $\times$5.6 mm display panel. The uniformity of the LED's output should be improved for display applications.

Moreover, it was interesting to measure the brightness of the whole micro display. The luminance of the μD as a function of the driving current was measured and is shown in Fig. 8. The brightness of the μD increased as the current increased but the performance of the EQE decreased as the

REFERENCES

[1] J. R. Bonar, G. J. Valentine, Z. Gong, J. Small, and S. Gorton, "High-brightness low-power consumption microLED arrays," in *Proc. SPIE*, vol. 9768, Mar. 2016, pp. 97680Y1–97680Y9.

[2] J. Day *et al.*, "III-Nitride full-scale high-resolution microdisplays," *Appl. Phys. Lett.*, vol. 99, no. 3, pp. 1–3, Jul. 2011.

[3] G. Chen *et al.*, "Performance of high-power III-nitride light emitting diodes," *Physica Status Solidi (A)*, vol. 205, no. 5, pp. 1086–1092, 2008.

[4] S. Pimputkar, J. S. Speck, S. P. DenBaars, and S. Nakamura, "Prospects for LED lighting," *Nat. Photon.*, vol. 3, no. 4, pp. 180–182, Apr. 2009.

[5] C. M. Kang *et al.*, "Fabrication of a vertically-stacked passive-matrix micro-LED array structure for a dual color display," *Opt. Exp.*, vol. 25, no. 3, pp. 2489–2495, Feb. 2017.

[6] H. X. Jiang, S. X. Jin, J. Li, J. Shakya, and J. Y. Lin, "III-Nitride blue microdisplay," *Appl. Phys. Lett.*, vol. 78, no. 9, pp. 1303–1305, Feb. 2001.

[7] K. Zhang, D. Peng, K. M. Lau, and Z. Liu, "Fully-integrated active matrix programmable UV and blue micro-LED display system on-panel (SoP)," *J. Display*, vol. 25, no. 4, pp. 240–248, 2017.

[8] W. C. Chong, W. K. Cho, Z. J. Liu, C. H. Wanga, and K. M. Lau, "1700 pixels per inch (PPI) passive-matrix micro-LED display powered by ASIC," in *Proc. IEEE Compd. Semicond. Integr. Circuit Symp.*, Oct. 2014, pp. 19–22.

[9] P. Tian *et al.*, "Characteristics and applications of micro-pixelated GaN-based light emitting diodes on Si substrates," *J. Appl. Phys.*, vol. 115, Jan. 2014, Art. no. 033112.

[10] M. Watanabe *et al.*, "Over 1000 channel nitride-based micro-light-emitting diode arrays with tunnel junctions," *Jpn. J. Appl. Phys.*, vol. 53, Apr. 2014, Art. no. 05FL06.

[11] J. Herrnsdorf *et al.*, "Active-matrix GaN micro light-emitting diode display with unprecedented brightness," *IEEE Trans. Electron Devices*, vol. 62, no. 6, pp. 1918–1925, Jun. 2015.

[12] R. H. Horng, K. C. Shen, Y. W. Kuo, and D. S. Wuu, "Effects of cell distance on the performance of GaN high-voltage light emitting diode," *Electrochem. Solid-State Lett.*, vol. 1, no. 5, pp. R21–R23, 2012.

[13] M.-C. Tseng *et al.*, "P-side-up thin-film AlGaInP-based light emitting diodes with direct ohmic contact of an ITO layer with a GaP window layer," *Opt. Exp.*, vol. 22, no. S7, pp. A1867–A1962, Dec. 2014.

[14] R.-H. Horng *et al.*, "Development and fabrication of AlGaInP-based flip-chip micro-LEDs," *IEEE J. Electron Devices Soc.*, vol. 6, pp. 475–479, Apr. 2018.

HUAN-YU CHIEN received the B.S. degree from the Department and Institute of Optoelectronic System Engineering, Hsinchu, Taiwan, in 2015, and the M.S. degree from the Graduate Institute of Precision Engineering, National Chung Hsing University, Taichung, Taiwan, in 2017. His major research focuses on high-voltage LED manufacturing process and simulation.

FU-GOW TARNTAIR received the B.S. degree in applied chemistry and the Ph.D. degree in electrical engineering from National Chiao Tung University, Hsinchu, Taiwan, in 1992 and 2000, respectively. He serviced in UMC Group, Hsinchu, from 2000 to 2016.

He is currently a Post-Doctoral Fellow with the Institute of Electronics, National Chiao Tung University under the guidance of Prof. R. H. Horng.

RAY-HUA HORNG (M'07–SM'11–F'15) received the B.S. degree in electrical engineering from National Cheng Kung University, Tainan, Taiwan, in 1987 and the Ph.D. degree in electrical engineering from National Sun Yat-sen University, Kaohsiung, Taiwan, in 1993.

She is currently a Distinguished Professor with the Institute of Electronics, National Chiao Tung University, Hsinchu, Taiwan. Her current research interests include solid-state lighting devices, solar cells, power device, HEMT, flexible electronics, optoelectronics, and nitride and oxide semiconductor MOCVD growths.

DONG-SING WUU (M'05–SM'16) received the B.S., M.S., and Ph.D. degrees in electrical engineering from National Sun Yat-sen University, Kaohsiung, Taiwan, in 1985, 1987, and 1991, respectively.

From 2010 to 2016, he served as the President of Da-Yeh University. He is currently a Distinguished Professor with the Department of Materials Science and Engineering, National Chung Hsing University, Taichung, Taiwan. His current research interests include nitride- and oxide-based materials, optical devices, and sensors.